Life Sciences 90 (2012) 365–372

Contents lists available at SciVerse ScienceDirect

Life Sciences

journal homepage: www.elsevier.com/locate/lifescie

Fructose-1,6-bisphosphate attenuates induction of nitric oxide synthase in microglia stimulated with lipopolysaccharide

Young-Chae Kim [a], Tae Yeop Park [a], Eunjoo Baik [a], Soo Hwan Lee [a,b,*]

[a] Department of Physiology, School of Medicine, Ajou University, Suwon 443-749, Republic of Korea
[b] Research Institute of Pharmaceutical Sciences and Technology, Ajou University, Suwon 443-749, Republic of Korea

ARTICLE INFO

Article history:
Received 13 July 2011
Accepted 13 December 2011

Keywords:
Fructose-1,6-bisphosphate (FBP)
Neuroprotection
Microglia
Nitric oxide (NO)
Mitogen-activated protein kinases (MAPKs)
Reactive oxygen species (ROS)

ABSTRACT

Aims: Fructose-1,6-bisphosphate (FBP) is a glycolytic intermediate with neuroprotective action in various brain injury models. However, the mechanism underlying the neuroprotection of FBP has not been fully defined. In this study, we investigated whether FBP inhibits endotoxin-induced nitric oxide (NO) production and inducible nitric oxide synthase (iNOS) expression in microglial cells and explored the possible mechanisms of the effects of FBP.
Main methods: Murine microglial cell line BV2 and primary cultured murine microglial cells were used. NO production and iNOS expression were determined by Griess reaction, RT-PCR and Western blot. Luciferase assay using iNOS promoter-luciferase (iNOS-Luc) construct was adopted for measuring transcriptional activity.
Key findings: FBP dose-dependently suppressed lipopolysaccharide (LPS)-induced NO production, along with reducing the expression of iNOS at both the protein and mRNA level in primary cultured murine microglia and BV2 cells. FBP significantly inhibited iNOS promoter activity but stabilized iNOS mRNA. Among transcription factors known to be related to iNOS expression, activator protein (AP-1) activation was significantly blocked by FBP. FBP suppressed LPS-induced phosphorylation of three MAPK subtypes-p38 MAPK, JNK and ERK. FBP inhibited LPS-induced production of reactive oxygen species (ROS) and decreased intracellular GSSG/GSH ratio.
Significance: Our findings suggest that FBP attenuates the LPS-induced iNOS expression through inhibition of JNK and p38 MAPK, which might be related to ROS downregulation.

Introduction

Inflammation is a widely accepted common denominator among various neuropathological processes and has been implicated as a critical mechanism responsible for the progression of neurodegeneration (Brown and Neher, 2010; Minghetti, 2005). Brain inflammation is characterized by glial cell activation accompanied by production of oxygen free radicals and other inflammation-related products that are toxic to neurons. Accumulating evidence has shown that induction of the inflammation-related enzymes such as inducible nitric oxide synthase (iNOS) and cyclooxgenase(COX)-2 are critical mechanisms by which inflammatory cells contribute to the development of cerebral damage under various pathologic conditions. Indeed, experiments using iNOS and COX-2 inhibitors suggest that inflammation-induced enzymes are potentially effective targets for the treatment or prevention of neuronal injury (Nogawa et al., 1997; Pannu and Singh, 2006; Sugimoto and Iadecola, 2002).

Fructose-1,6-bisphosphate (FBP) is a glycolytic intermediate which has a neuroprotective effect in various brain injury models (Izumi et al., 2003; Kaakinen et al., 2006; Park et al., 2004; Stringer and Xu, 2008; Vexler et al., 2003). The neuroprotection by FBP has been attributed to the maintenance of ATP levels (Cardenas et al., 2000; Espanol et al., 1998) and the reduction of glutamate (Bickler and Buck, 1996) and oxidative stress (Park et al., 2004; Vexler et al., 2003). Other possible mechanisms have also been suggested, including calcium chelation (Bickler and Kelleher, 1992), antagonism of NMDA receptors (Izumi et al., 2003) and modulation of second messenger systems (Donohoe et al., 2001; Fahlman et al., 2002; Song et al., 2005). However, mechanisms whereby FBP protects the brain have not been fully elucidated yet.

In this context, it is important to note that FBP has anti-inflammatory and immunomodulatory effects, though underlying mechanisms of its action have not been well understood. FBP ameliorates carrageenan-induced pleurisy (Alves-Filho et al., 2004) and suppresses T-cell proliferation (Cohly et al., 2004; Lopes et al., 2006). In addition, FBP is known to inhibit the production of inflammatory mediators, including cytokines (Cohly et al., 2004; Tamaki et al., 2002), prostaglandin E_2 (PGE_2) (Ahn et al., 2002) and nitric oxide (NO) (Cardenas et al., 2000; Edde et al., 1998). These data provide insight

* Corresponding author at: Department of Physiology, Ajou University School of Medicine, #5, Wonchon-dong, Suwon, 443-749, Republic of Korea. Tel.: +82 31 219 5043; fax: +82 31 219 5049.
E-mail address: shwanlee@ajou.ac.kr (S.H. Lee).

0024-3205/$ – see front matter © 2011 Elsevier Inc. All rights reserved.
doi:10.1016/j.lfs.2011.12.011

into the inference that the anti-inflammatory effects could be implicated in the neuroprotective actions of FBP. Thus, in this study, in order to better understand the neuroprotective mechanism of FBP in situations related to brain disease, we investigated whether FBP inhibits endotoxin-induced NO production and iNOS expression in microglial cells and explored the possible mechanisms of the effects of FBP.

Materials and methods

Chemicals

D-fructose-1,6-bisphosphate (FBP), N-acetylcysteine (NAC), 6-hydroxy-2,5,7,8-tetramethylchroman-2-carboxylic acid (Trolox), pyrrolidine dithiocarbamate (PDTC), actinomycin D and lipopolysaccharide (LPS) were purchased from Sigma (St. Louis, MO). MAPKs inhibitors, such as SP600125 (JNK inhibitor), PD98059 (ERK inhibitor), and SB202190 (p38 inhibitor), were obtained from Calbiochem (San Diego, CA). [α-^{32}P] dCTP was purchased from DuPont-NEN (Boston, MA).

Cell cultures

BV2 cells, the murine microglial cell line originally developed by Dr. V. Bocchini at University of Perugia (Blasi et al., 1990), were generously provided by Dr. E.H. Joe at Ajou University (Suwon, Korea). The cells were maintained in Dulbecco's modified Eagle's medium (DMEM, Life Technologies, Gaithersburg, MD) supplemented with 10% FBS (Invitrogen, Carlsbad, CA) and 100 U/ml penicillin/streptomycin at 37 °C in a humidified incubator with 5% CO_2.

Primary murine microglial cell isolation

Primary microglia cell cultures were prepared from prenatal day 1–2 ICR mouse (Daehan Biolink, Korea) brains. Briefly, the neonatal mouse was anesthetized with ethyl ether. And the cortices were mechanically dissociated with a flamed-polished Pasteur pipette in MEM supplemented with 20 mM glucose. Cell were plated on 6 or 24 multiwell plates with culture medium supplemented with 10% fetal bovine serum, and 0.01 μg/ml epidermal growth factor (Sigma, St. Louis, MO) for 24 h. The medium was changed every 3 days after seeding. The cells reached to confluence on day 14. 14-day mixed glial cell cultures were agitated on an orbital shaker for 4 h at 250 rpm at 37 °C. The supernatant was collected, and microglia were filtered through a 32-μm nylon mesh. Microglia were incubated on uncoated petri dishes in a moist 10% CO_2 atmosphere for 20 min at 37 °C to allow microglia cells to attach.

Nitric oxide (NO) assay

NO production was determined by measuring nitrite, a stable oxidation product of NO, as described previously (Green et al., 1982). Nitrite concentration in the medium was spectrophotometrically measured by Griess reaction. The culture medium was mixed with an equal volume of Griess reagent (0.1% naphthyl-ethylenediamine hydrochloride and 1% sulfanilamide in 10% phosphoric acid) and incubated at room temperature for 10 min. Absorbance was measured at 540 nm in a microplate reader (Molecular Devices, Sunnyvale, CA). Sodium nitrite was used as a standard.

Reverse transcription and polymerase chain reaction (RT-PCR) for iNOS

Total RNA was extracted from the samples with Easy-blue kit® (Intron, Seoul, Korea) according to the manufacturer's protocol. Aliquots of total RNA (1 μg) were transcribed using AMV reverse transcriptase (Boehringer Mannheim, Indianapolis, IN). Primer sequences were as follows: iNOS, sense, 5′-CGTGTGCCTGCTGCCTTCCTGCTGT-3′; antisense, 5′-GTAATCCTCAACCTGCTCCTCACTC-3′; GAPDH, sense, 5′-GTGAAGGTCGGTGTGAACGGATTT-3′; antisense, 5′-CACAGTCTTC TGAGTG GCAGTGAT-3′.

PCR amplification of the resulting cDNA template was conducted using the following conditions: iNOS; 28 cycles of denaturing at 94 °C for 1 min, annealing at 60 °C for 1 min, and extension at 72 °C for 1 min; GAPDH; 30 cycles of denaturing at 94 °C for 0.5 min, annealing at 60 °C for 0.5 min, and extension at 72 °C for 1 min. Reaction products were then separated on a 2% agarose gel and photographed under ultraviolet light. The optical density was determined by a Gel doc system (GEL DOC 2000, Bio-Rad, Hercules, CA).

Western blot analysis

Western blot analysis was used to determine the expression of iNOS expression and the activation of MAPKs. After treatment, cell lysates were prepared by scraping BV2 cells in the lysis buffer (Tris 50 mM at pH 7.4, 10 mM EDTA, 1% Tween-20, 10 μM leupeptin, and 1 mM phenylmethyl-sulfonyl fluoride) and sonicating for 10–15 s (20-W pulses). Cell lysates containing equal amounts of protein were subjected to a 10% SDS-PAGE. Proteins were transferred to nitrocellulose membranes and subsequently blocked in T-TBS buffer (20 mM Tris buffer; 0.5 M NaCl, 0.5% Tween-20) containing 5% nonfat dried milk. Blots were incubated with polyclonal anti-iNOS (Upstate biotechnology, Lake Placid, NY, 1:2,000), MAPKs (Cell Signaling Technology, Danvers, MA, 1:1,000) or GAPDH antibody (Santa Cruz Biotechnology, Santa Cruz, CA), and followed by incubation with a horse radish peroxidase-labeled secondary antibody (Santa Cruz Biotechnology, 1:10,000). The blots were visualized using an ECL chemiluminescence detection kit (Amersham Biosciences, Piscataway, NJ).

Luciferase assay

Luciferase assay was carried out using a kit from Promega (Madison, WI). piNOS-luc reporter construct, which contains the murine iNOS promoter in pGL3 vector was provided by Dr. D. Hwang at UC Davis, USA. Cells in 24 well plates were transfected with piNOS-Luc and pCMV-β-gal plasmid as an internal control using Lipofectamine™ 2000 reagent (Invitrogen Carlsbad, CA) for 24 h and transfected-cells were treated with different agents (triplicate wells each) for 5 h. Cells were then lysed by adding 100 μl of lysis buffer, sonicated for 10 s and centrifuged in a tabletop microcentrifuge. An aliquot (20 μl) was mixed with 100 μl of assay reagent, vortexed, and read immediately in a TD20/20 luminometer (Turner Biosystems, Sunnyvale, CA). The luciferase activity was normalized with β-galactosidase activity and expressed as % of treatment-free control.

Electrophoretic mobility shift assay (EMSA)

Nuclear proteins (10 μg) were used for the electrophoretic mobility shift assay for the detection of the DNA binding activity of AP-1, NF-κB, CREB, and C/EBP. DNA-protein binding reactions were performed at room temperature for 20 min in 20 mM HEPES-KOH, pH 7.9; 10% glycerol, 420 mM NaCl, 0.2 mM EDTA, 1.5 mM $MgCl_2$, 0.5 mM PMSF, 0.5 mM DTT and 10 μM leupeptin, plus 1 μg of poly (dI-dC) and ~0.3 pmol of labeled double-stranded sequences for AP-1, NF-κB, CREB or C/EBP binding. The following oligonucleotides were synthesized by Bioneer (Daejeon, Korea) and labeled with [α-^{32}P] dCTP (3,000 Ci/mmol, 250 μCi/25 μl); 5′-AGCTTGGGGACTTTCC-3′, containing a binding site for NF-κB complexes; 5′-CGCTTGATGAGTCAGCCGGAA-3′, containing a binding site for AP-1 complexes; 5′-GATCGTCACCACTACGTCACGTGGAGTCCGCTT-5′, containing a binding site for CRE/E-box complexes; and 5′-GATCCTGCCGCTGCGGTTCTTGCGCAACTCACT-3′ containing a binding site for CREB complexes. The DNA-protein complexes were resolved on an 8% polyacrylamide

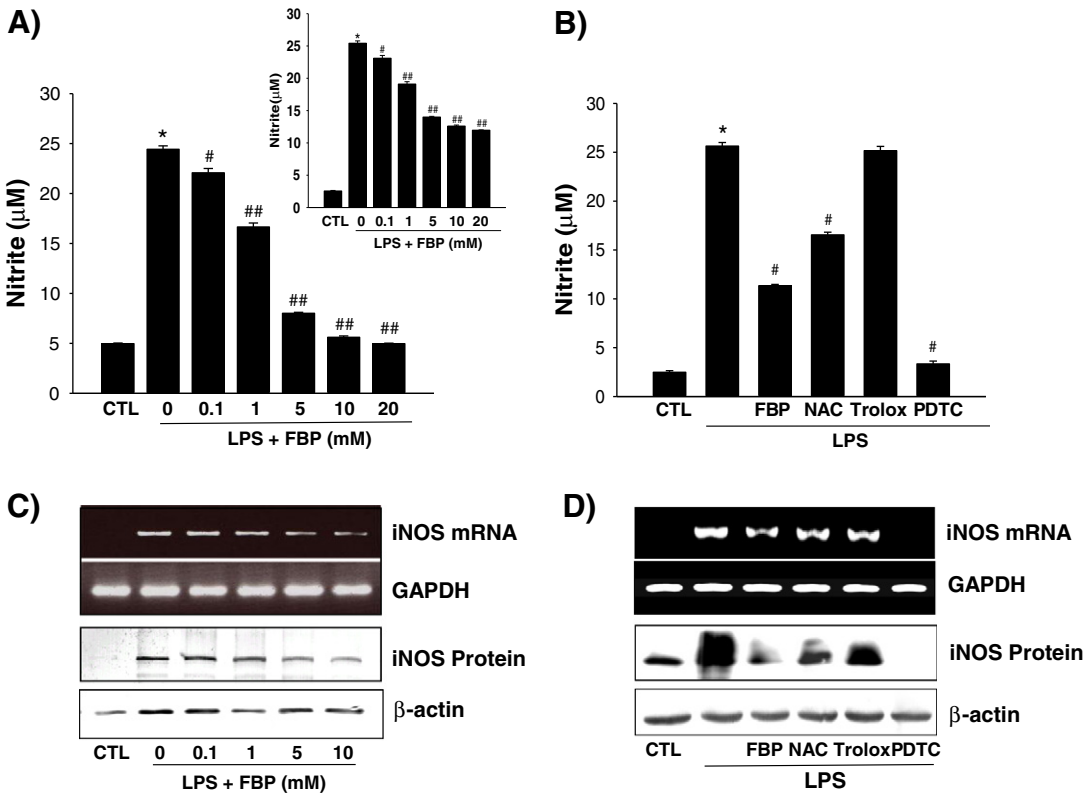

Fig. 1. Effects of FBP on LPS-induced NO production and iNOS expression in BV2 microglial cells. Cells were incubated with LPS (1 μg/ml) for indicated time. FBP and antioxidants including N-acetylcystein (NAC, 10 mM), trolox (10 μM) and PDTC (50 μM) were added 30 min prior to LPS exposure. (A), (B) After 48 h, accumulated levels of NO in the media were measured by Griess reaction as described in the Experimental Procedure. Data obtained from primary murine microglial cells are shown in inset of (A). The data represent the mean ± S.E. from at least three independent experiments. *$p<0.01$ vs. control (CTL). #$p<0.05$, ##$p<0.01$ vs LPS alone. (C), (D) Levels of iNOS mRNA and protein were determined by RT-PCR and Western blot as described in the Materials and methods at 4 h and 24 h, respectively.

gel containing in 0.25 × TBE (1 × TBE: 90 mM Tris borate, 2 mM EDTA, pH 8.0). The gel was run at 200 V for 2 h at 5 °C. Gels were then dried and subjected to autoradiography at −80 °C with Kodak TGM/RA film.

Measurement of ROS release

Intracellular ROS was measured fluorometrically using the non-fluorescent dye, 2′,7′-dichlorofluorescein diacetate (DCF-DA), which easily permeates cells and is hydrolyzed to fluorescent 2′,7′-dichlorofluorescein (DCF) upon interaction with intracellular ROS. Cells were loaded with 20 μM of DCF-DA and 20% Pluronic F-127 for 30 min and then washed with HCSS. The DCF fluorescence was analyzed using a fluorescence plate reader (Luminescence spectrometer-55, Perkin Elmer, Wellesley, MA) at an excitation of 490 nm and an emission of 530 nm.

GSSG/GSH assay

Total glutathione (GSH plus GSSG) was determined by photometric determination of 5-thio-2-nitrobenzoate, formed from 5,5′-dithiobis(2-nitrobenzoic acid, DTNB) at 405 nm according to the protocol of Akerboom and Sies (1981). The assay mixture was 0.1 M sodium phosphate buffer (pH 7.5) containing 1 mM EDTA, 0.3 mM 5,5′-dithio-bis(2-nitrobenzoic acid), 0.4 mM NADPH, and 1 U/ml glutathione reductase and 10 μl of cell lysate. The increase in absorbance at 405 nm was monitored at 15 s intervals for 2.5 min using a micro plate reader (VERSAmax, Molecular Device, Sunnyvale, CA). GSSG was quantified after derivatizing GSH in the sample with 2-vinylpyridine for 1 h. After incubation, 10 μl of the each sample was assayed as described above using similarly treated GSSG standards (0–5 μM).

Statistics

The data are expressed as the mean ± S.E. from four independent experiments. An analysis of variance (ANOVA) followed by Dunnet's multiple comparison tests was used for statistical comparisons. A value of $p<0.05$ was considered to be significant (Sigma Stat, Jandel Scientific, Chicago, IL).

Results

Fructose 1,6-biphosphate (FBP) reduces bacterial lipopolysaccharide (LPS)-induced NO production and iNOS expression

In order to characterize the nature of the anti-inflammatory action of FBP, we examined its effects on the production of NO in BV2 microglial cells. When treated with LPS at concentrations up to 1 μg/ml for 24 h, microglial cells released NO in a concentration-dependent manner. Thus, cells were stimulated with 1 μg/ml of LPS in the subsequent experiments. LPS reduced the cell viability by 24% compared to the control group. Recovery of cell viability was observed upon treatment with FBP, and a maximal effect of FBP was observed at 10 mM (105.5 ± 2.7% of control). FBP reduced the accumulated levels of NO in the media in a dose-dependent manner when added to the culture media 30 min prior to LPS stimulation (Fig. 1A). The inhibitory effect of FBP on NO production was maximal at 10 mM. Experiments with primary cultured mouse microglia showed similar results (Fig. 1A inset). LPS-induced iNOS expression was significantly suppressed by FBP at both the mRNA and the protein level (Fig. 1C). Antioxidants, such as N-acetylcysteine (NAC, 10 mM) and pyrrolidine dithiocarbamate (PDTC, 50 μM) attenuated LPS-induced NO production and iNOS expression (Fig. 1B, D). The effect of FBP on both the protein

and mRNA levels of iNOS could be due to decreased transcription and/or reduced mRNA stability. FBP significantly inhibited LPS-induced transcriptional activation of the iNOS promoter (Fig. 2A, 285.0 ± 9.0% and 115.1 ± 6.1% of control in LPS alone and LPS plus FBP (10 mM), respectively). To examine the stability of iNOS mRNA, actinomycin D was added to cells after 4 h of LPS treatment and the level of iNOS mRNA was measured from the time of addition up to 8 h. The iNOS transcript completely decayed by 8 h of post-actinomycin D treatment. The mRNA decay was significantly reversed by treatment with FBP (Fig. 2B).

Effects of FBP on DNA binding of transcription factors

Previous studies have suggested that various transcription factors, such as nuclear factor-kappa B (NF-κB), cAMP response element-binding protein (CREB), activator protein (AP-1) and CCAAT/enhancer binding protein (C/EBP), are important regulators of the expression of iNOS gene expression (Kleinert et al., 2004). The DNA binding activities of all these transcription factors increased upon LPS treatment in microglial cells. FBP diminished the binding of AP-1, but did not affect DNA binding of NF-κB, CREB and C/EBP (Fig. 3). Antioxidants, such as NAC (10 mM) and PDTC (50 μM), also attenuated AP-1 binding activity. Binding of these transcription factors to specific DNA sites

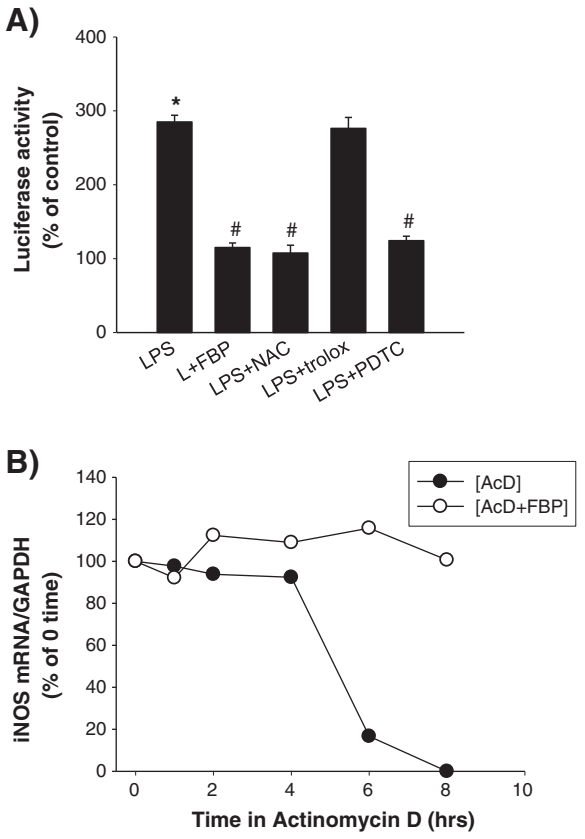

Fig. 2. Effects of FBP on the trasnscriptional activation of the iNOS promotor and the stability of iNOS mRNA. (A) Cells were transfected with iNOS-Luc for 24 h and treated with LPS (1 μg/ml) for 5 h. FBP (10 mM), N-acetylcystein (NAC, 10 mM), trolox (10 μM) or PDTC (50 μM) were added 30 min prior to LPS exposure. The luciferase activity was measured as described in Materials and methods and normalized with β-galactosidase activity. Values were expressed as % of treatment-free control. The data represent the mean ± S.E. from at least three independent experiments. *$p<0.01$ vs. control (CTL). #$p<0.01$ vs LPS alone. (B) Cells were incubated with LPS (1 μg/ml) for 4 h and washed three times with PBS (pH 7.2). Cells were further incubated in fresh media containing actinomycin D (AcD) at a concentration of 0.5 μg/ml in the absence or presence of FBP (10 mM). Total RNA was extracted at the indicated times and the level of iNOS mRNA was determined by RT-PCR. Data are expressed as the percent of a ratio of iNOS mRNA compared to GAPDH at the time of AcD addition. The graph shows the representative result of 3 independent experiments.

was blocked completely or almost completely by a 100-fold excess of the related unlabelled probes, indicating that binding was specific.

FBP inhibited LPS-induced iNOS expression by blocking JNK/p38 MAPK

MAPK signaling pathways play a critical role in the regulation of inflammatory response and the coordination of the induction of various inflammatory mediators (Guha and Mackman, 2001). As shown in Fig. 4A, LPS markedly induced the phosphorylation of JNK, ERK and p38 kinase, and FBP suppressed LPS-induced phosphorylation of all of these MAPKs.

To determine which MAPK signaling pathway is involved in LPS-induced iNOS expression, cells were pretreated for 30 min with MAPK-specific inhibitors (PD98059 for MEK1/2, SB203580 for p38 kinase and SP600125 for JNK) before exposure to LPS. SP60015 and SB203580 significantly inhibited LPS-induced iNOS expression and NO production, while PD98059 showed minimal effect, if any (Fig. 4B and C). These data suggest that LPS-induced iNOS expression appears to be regulated by JNK and p38 kinase, but not by ERK in BV2 microglial cells. Thus, the suppression of JNK and p38 kinase phosphorylation may be associated with the inhibitory effect of FBP on iNOS expression.

The involvement of the MAPK pathway in regulating LPS-mediated iNOS expression has been hypothesized to be redox-dependent (Kim et al., 2004; Pawate et al., 2004). In the present study, we also observed that antioxidants, NAC (10 mM) and PDTC (50 μM), inhibited LPS-induced phosphorylation of JNK and p38 kinase (Fig. 4A) and reduced NO production (25.6 ± 0.4 and 16.6 ± 0.3 μM in the LPS control and in the NAC treated cells, respectively).

FBP reduces LPS-induced ROS production

In order to determine whether FBP reduces oxidative stress under our experimental conditions, we measured the fluorescence intensity of 2′,7′-dichlorofluorescein (DCF), an oxidant sensitive dye, and the cellular oxidized glutathione (GSSG) to reduced glutathione (GSH) ratio. The fluorescence intensity of each sample was expressed as the percentage over the vehicle-treated control. The level of ROS increased in a time-dependent manner, peaking at 4 h after LPS treatment. FBP reduced LPS-induced ROS production (Fig. 5A) and also decreased the cellular GSSG/GSH ratio at 4 h after stimulation (Fig. 5B).

Discussion

The present study shows that FBP inhibits the induction of NO production and diminished iNOS expression in BV2 microglia exposed to LPS. FBP has been known to inhibit iNOS expression in oxygen-glucose-deprived (OGD) rat forebrain slices (Cardenas et al., 2000) and macrophages stimulated with LPS (Edde et al., 1998). However, the underlying mechanism of FBP action has not yet been elucidated in detail. Previous reports have shown that the expression of iNOS is regulated at the transcriptional and posttranscriptional levels (Amin et al., 1997; Nathan and Xie, 1994). Our results show that FBP hindered LPS-induced transcriptional activation of the iNOS promoter (Fig. 2A). Among the tested transcription factors activated by LPS, only AP-1 binding activity was attenuated by FBP (Fig. 3). Though NF-κB is the most important transcription factor in LPS-induced transcriptional activation of iNOS, FBP did not affect NF-κB binding in our study. This result coincides with a previous study showing that FBP did not affect NF-κB binding activity in macrophages stimulated with LPS (Edde et al., 1998). Based on this result, they speculated that FBP might enhance iNOS mRNA degradation in macrophages. However, our results indicate that this is not the case at least in BV2 microglial cells. FBP increased the stability of the iNOS transcript in microglia, which apparently conflicts with above data supporting the inhibitory effect of FBP at transcriptional level.

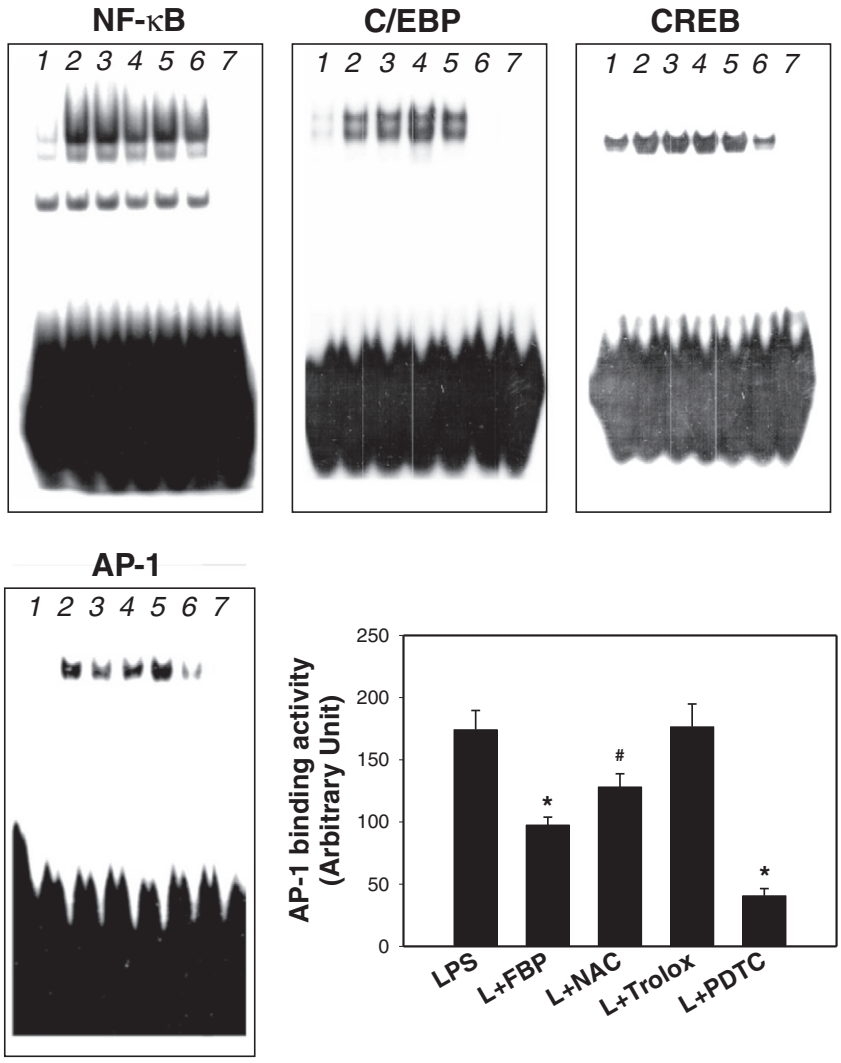

Fig. 3. Effects of FBP on DNA binding of transcription factors. BV2 cells were incubated with LPS (1 μg/ml) for 15 min for NF-κB or 2 h for C/EBP, CREB and AP-1. FBP (10 mM), N-acetylcystein (NAC, 10 mM), trolox (10 μM) or PDTC (50 μM) were added 30 min prior to LPS exposure. Nuclear proteins were extracted at the indicated times and the DNA binding activities of the transcription factors were determined by electrophoretic mobility shift assay. Lane 1: control; Lane 2: LPS alone; Lane 3: LPS + FBP (10 mM); Lane 4: LPS + NAC (10 mM); Lane 5: LPS + trolox (10 μM); Lane 6: LPS + PDTC (50 μM); Lane 7: cold oligonucleotide. Bar graph represents the mean ± S.E. from three independent experiments. *$p<0.01$ vs. LPS alone. #$p<0.05$ vs LPS alone.

However, our data clearly shows that FBP reduces the total levels of iNOS mRNA induced by LPS. Thus, it is strongly suggested that transcriptional effect of FBP is the main one in determining iNOS mRNA levels under our experimental condition.

MAPK signaling pathways are well known to be critically involved in the iNOS gene expression. In the present study, we observed that specific inhibitors of JNK and p38 kinase inhibited LPS-induced production of NO and the expression of iNOS. These data suggest key roles for these kinase cascades in LPS-induced microglial activation. However ERK kinase did not seem to be involved in the LPS-induced iNOS gene expression (Fig. 4). These results are in accordance with a previous report suggesting p38 kinase, but not ERK kinase, is an important mediator of iNOS induction by LPS in BV2 microglia (Han et al., 2002). In addition, these results are supported by the fact that the promoter regions of the genes encoding iNOS have binding site for the JNK-dependent transcription factor AP-1. Indeed, FBP suppressed LPS-induced phosphorylation of all three MAPKs and AP-1 binding activity. Taken together, these data suggest that the suppression of JNK and p38 MAPK phosphorylation might be associated with the inhibitory effect of FBP on LPS-induced iNOS gene expression. However, it should be pointed out that there are some inconsistent reports on the role of MAPKs in iNOS gene expression. Though our findings are consistent with a previous study of C-6 glioma cells in terms of dissociation of ERK activation and iNOS expression (Nishiya et al., 1997), they differ from those of other studies with myocytes (Singh et al., 1996), primary rat microglial cells (Bhat et al., 1998) and even BV2 microglia (Bae et al., 2006), in which ERK pathway is involved in the expression of iNOS. These contradictions probably stem from the well-known, but not well-understood, complex regulation of iNOS gene expression, which is cell type-, species-, and stimulus-specific.

Accumulating evidence indicates that oxidative components contribute to LPS-induced iNOS expression (Kim et al., 2004; Pawate et al., 2004). Indeed, several putative sequences for ROS sensitive transcription factors have been identified in the 5′-upstream region of the iNOS gene, including sites for NF-κB, NF-IL6 and AP-1 (Kleinert et al., 2004). Consequently, the management of cellular ROS levels could be regarded as a key to the regulation of iNOS expression. FBP has been shown to suppress ROS production by neutrophils, keratinocytes and cortical neurons and preserve the antioxidative capacities in cortical neurons and skin during oxidative stress (Ahn et al., 2002, 2007; Park et al., 2004). In the present study, we show that FBP reduced ROS production and maintained glutathione in microglia during LPS stimulation. FBP is known to suppress

in vitro hydroxyl radical generation in Fenton reaction (Tang et al., 2008) and also preserve cellular antioxidative capacity by stimulating the pentose phosphate pathway (PPP) (Vexler et al., 2003). In addition, we reported that FBP reduced NMDA-induced ROS production by downregulation of the phosphorylation of ERK and p38 kinase in cortical neurons (Park et al., 2004). Thus, together with the suppressive effects of antioxidants, such as NAC and PDTC, against NO production and phosphorylation of MAPKs (Fig. 4), these results support the inference that the antioxidative property of FBP is associated with inhibition of MAPKs and thereby attenuation of iNOS expression in microglia exposed to LPS.

FBP has been reported to have neuroprotective effects in various brain injury models, including hypoxia–ischemia (Farias et al., 1990; Kaakinen et al., 2006; Kuluz et al., 1993; Sola et al., 1996; Trimarchi et al., 1997; Vexler et al., 2003), seizure (Stringer and Xu, 2008), β-amyloid induced neurotoxicity (Song et al., 2005) and insulin-induced hypoglycemia (Farias et al., 1989). One of the main hypotheses for these effects is that FBP serves as a glycolytic intermediate and alters metabolic production of ATP under pathologic conditions (Bickler and Buck, 1996; Cardenas et al., 2000; Espanol et al., 1998; Hardin and Roberts, 1994; Juergens and Hardin, 1996). In support of this hypothesis, recent report demonstrated that the levels of FBP significantly increased in brain after intraperitoneal and oral administration and exogenous FBP was taken up into cells within brain and not trapped in the endothelial cells of the brain (Xu and Stringer, 2008). It was shown that FBP could cross lipid bilayers by passive diffusion (Ehringer et al., 2000) or via a dicarboxylate transport system (Hardin et al., 2001).

In contrast, several other reports showed FBP failed to preserve ATP in in vivo and in vitro models of hypoxia or ischemia (Hofer et al., 2009; Kelleher et al., 1995; Liu et al., 2008). It was speculated that the lack of its effect on energy metabolism was probably because it was prevented from entering cells in adequate quantities. On the basis of these results, it has been suggested that mechanisms other than augmented carbohydrate metabolism are responsible for previous reports of neuronal protection by FBP (Hofer et al., 2009). Indeed, the protective role of FBP has been attributed to a variety of mechanisms such as the reduction of glutamate (Bickler and Buck, 1996),

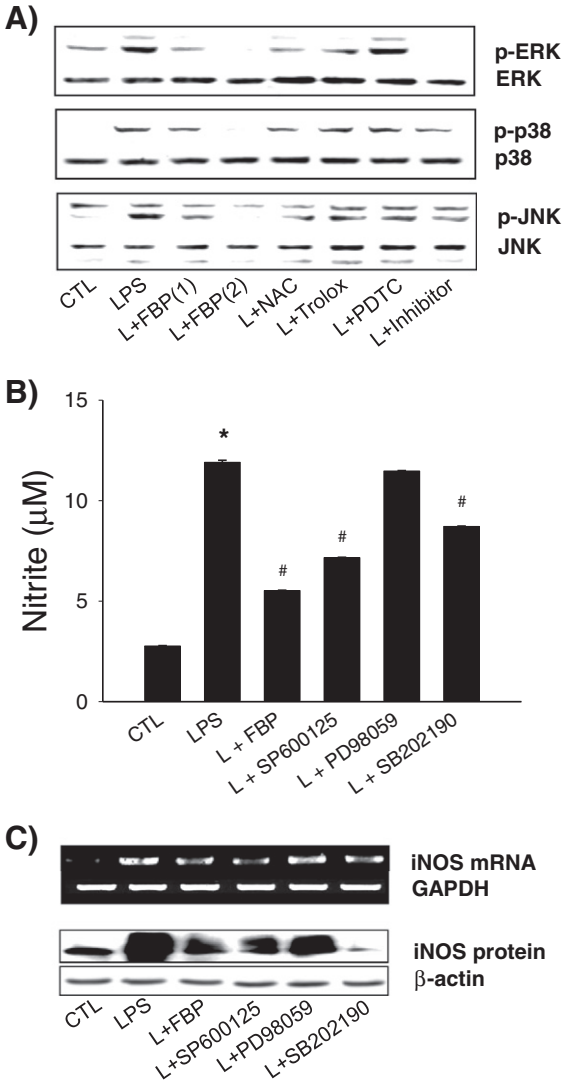

Fig. 4. Effects of FBP on the phosphorylation of MAPKs. (A) BV2 cells were incubated with LPS (1 μg/ml) for 15 min following pretreatments for 30 min with 10 mM of FBP(1) or antioxidants and subjected to immunoblot analysis using antibodies that specifically recognize phosphorylated and non-phosphorylated ERK, p-38 MAPK and JNK. In one group, cells were simultaneously treated with LPS and 10 mM of FBP (2). Applied antioxidants were NAC (10 mM), trolox (10 μM) and PDTC (50 μM). (B) Cells were incubated with LPS (1 μg/ml) following pretreatment for 30 min with 10 mM of FBP, 10 μM of PD98059, 10 μM of SB202190 or 4 μM of SP600125. After 48 h, accumulated levels of NO in the media were measured by Griess reaction as described in the Materials and methods. The data represent the mean ± S.E. from at least four independent experiments. *p<0.01 vs. control (CTL). #p<0.05 vs LPS alone. (C) Levels of iNOS mRNA and protein were determined by RT-PCR and Western blot as described in the Materials and Methods at 4 h and 24 h, respectively.

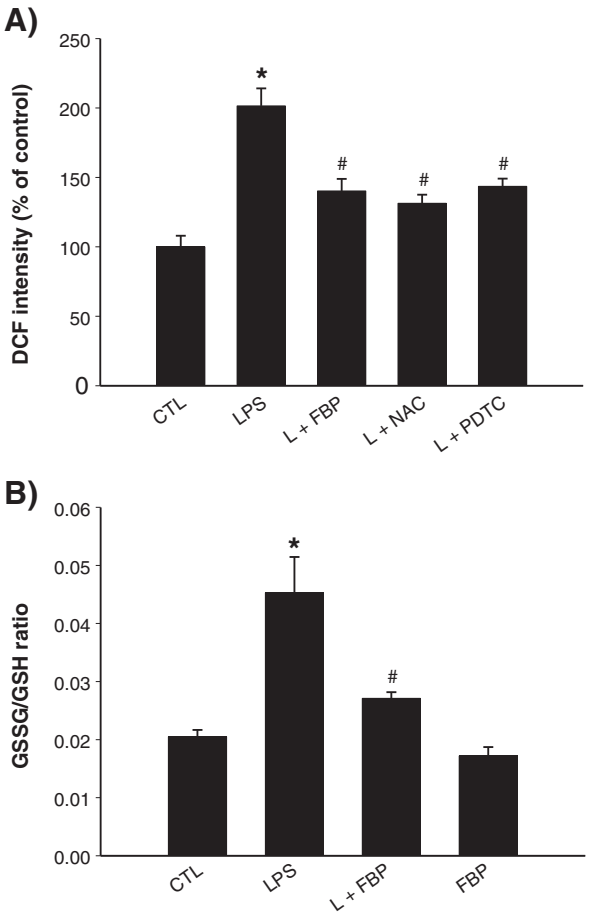

Fig. 5. Effects of FBP on LPS-induced oxidative stress in BV2 cells. (A) Cells were incubated with LPS (1 μg/ml) for 4 h. FBP (10 mM), N-acetylcystein (NAC, 10 mM), trolox (10 μM) and PDTC (50 μM) were added 30 min prior to LPS exposure. Intracellular levels of ROS were determined by fluorescence intensity of 2′,7′-dichlorofluorescein (DCF). (B) The cellular GSSG/GSH ratio was determined by DTNB reaction at 1 h of incubation with FBP (10 mM) in the presence or absence of LPS (1 μg/ml). The data represent the mean ± S.E. from at least four independent experiments. *p<0.01 vs. control (CTL). #p<0.05 vs LPS alone.

the mitigation of oxidative stress (Park et al., 2004; Vexler et al., 2003), calcium chelation (Bickler and Kelleher, 1992) and antagonism of NMDA receptors (Izumi et al., 2003). In addition, FBP initiates a series of neuroprotective signals, including phospholipase C (PLC) activation and increased activity of the MEK/ERK signaling pathway (Fahlman et al., 2002; Song et al., 2005) and up-regulates the expression of APE/Ref-1, an enzyme responsible for the repair of DNA (Long et al., 2002). Most of these regulatory processes would be expected to require lesser concentrations of FBP compared to the provision of substrate for energy metabolism (Hofer et al., 2009). Regardless of whether FBP has an extra- or intracellular site of action, currently a matter of controversy, accumulated evidence indicates that FBP has cytoprotective effects under various pathological conditions.

Induction of iNOS has been implicated in the pathogenesis of brain injury (del Zoppo et al., 2000; Ono et al., 2010; Pannu and Singh, 2006). Indeed, experiments have shown that selective inhibitors of iNOS are effective in preventing ischemic injury in brain (ArunaDevi et al., 2010; Cardenas et al., 1998; Greco et al., 2011). In this context, it was suggested that FBP might abolish iNOS expression by reducing glutamate release in oxygen-glucose-deprived rat forebrain slices and the beneficial effects of FBP were possibly associated with decreased production of NO (Cardenas et al., 2000). These results were obtained from organotypic slice culture and there was no description of the specific cell types therein involved. Activated microglia are involved in the progression of brain injury and neuroinflammation mediated by microglia has been regarded as a pathological hallmark of various CNS disorder (Brown and Neher, 2010). However, until this time, there has been no report describing the effect of FBP on microglial cells. Our data clearly showed that FBP could directly affect microglia and attenuate the LPS-induced iNOS. To our knowledge, our study is the first report to focus on microglial activation, and thereby adding the attenuation of neuroinflammation to the repertoire of neuroprotective mechanism of FBP.

Conclusion

In this study, we showed FBP, a glycolytic intermediate, exerts anti-inflammatory effect by inhibiting LPS-induced NO production and iNOS expression in microglial cells. This effect is mediated by suppression of JNK and p38 MAPK, which might be related to ROS downregulation. This study suggests that the attenuation of microglial activation and in turn, neuroinflammation is implicated in the neuroprotective mechanism of FBP.

Conflict of interest statement

The authors declare that there are no conflicts of interest.

Acknowledgments

This work was supported by a grant from of the “GRRC Program” of Gyunggi-Do, Republic of Korea through the Center for Cell Death Regulating Biodrug, Ajou University, Republic of Korea.

References

Ahn SM, Hwang JS, Lee SH. Fructose 1,6-diphosphate alleviates UV-induced oxidative skin damage in hairless mice. Biol Pharm Bull 2007;30:692–7.
Ahn SM, Yoon HY, Lee BG, Park KC, Chung JH, Moon CH, et al. Fructose-1,6-diphosphate attenuates prostaglandin E2 production and cyclo-oxygenase-2 expression in UVB-irradiated HaCaT keratinocytes. Br J Pharmacol 2002;137:497–503.
Akerboom TP, Sies H. Assay of glutathione, glutathione disulfide, and glutathione mixed disulfides in biological samples. Methods Enzymol 1981;77:373–82.
Alves-Filho JC, Santos RC, Castaman TA, de Oliveira JR. Anti-inflammatory effects of fructose-1,6-bisphosphate on carrageenan-induced pleurisy in rat. Pharmacol Res 2004;49:245–8.
Amin AR, Patel RN, Thakker GD, Lowenstein CJ, Attur MG, Abramson SB. Post-transcriptional regulation of inducible nitric oxide synthase mRNA in murine macrophages by doxycycline and chemically modified tetracyclines. FEBS Lett 1997;410:259–64.
ArunaDevi R, Ramteke VD, Kumar S, Shukla MK, Jaganathan S, Kumar D, et al. Neuroprotective effect of s-methylisothiourea in transient focal cerebral ischemia in rat. Nitric Oxide 2010;22:1-10.
Bae JH, Jang BC, Suh SI, Ha E, Baik HH, Kim SS, et al. Manganese induces inducible nitric oxide synthase (iNOS) expression via activation of both MAP kinase and PI3K/Akt pathways in BV2 microglial cells. Neurosci Lett 2006;398:151–4.
Bhat NR, Zhang P, Lee JC, Hogan EL. Extracellular signal-regulated kinase and p38 subgroup of mitogen-activated protein kinases regulate inducible nitric oxide synthase and tumor necrosis factor-a gene expression in endotoxin-stimulated primary glial cultures. J Neurosci 1998;18:1633–41.
Bickler P, Buck LT. Effects of fructose-1,6-bisphosphate on glutamate release and ATP loss from rat brain slices during hypoxia. J Neurochem 1996;67:1463–8.
Bickler PE, Kelleher JA. Fructose-1,6-bisphosphate stabilizes brain intracellular calcium during hypoxia in rats. Stroke 1992;23:1617–22.
Blasi E, Barluzzi R, Bocchini V, Mazzolla R, Bistoni F. Immortalization of murine microglial cells by a v-raf/v-myc carrying retro-virus. J Neuroimmunol 1990;27:229–37.
Brown GC, Neher JJ. Inflammatory neurodegeneration and mechanisms of microglial killing of neurons. Mol Neurobiol 2010;41:242–7.
Cardenas A, De Alba J, Moro MA, Leza JC, Lorenzo P, Lizasoain I. Neuroprotective effect of 1400W, a selective inhibitor of inducible nitric oxide synthase, in rat fore brain slices exposed to oxygen and glucose deprivation. Eur J Pharmacol 1998;354:161–5.
Cardenas A, Hurtado O, Leza JC, Lorenzo P, Bartrons R, Lizasoain I, et al. Fructose-1,6-bisphosphate inhibits the expression of inducible nitric oxide synthase caused by oxygen-glucose deprivation through the inhibition of glutamate release in rat forebrain slices. Naunyn Schmiedebergs Arch Pharmacol 2000;362:208–12.
Cohly H, Jenkins J, Skelton T, Meydrech E, Markov AK. Fructose-1,6-diphosphate suppresses T-lymphocyte proliferation, promotes apoptosis and inhibits interleukins-1, 6, beta-actin mRNAs, and transcription factors expression. Immunol Invest 2004;33:407–21.
del Zoppo G, Ginis I, Hallenbeck JM, Iadecola C, Wang X, Feuerstein GZ. Inflammation and stroke: putative role for cytokines, adhesion molecules and iNOS in brain response to ischemia. Brain Pathol 2000;10:95-112.
Donohoe PH, Fahlman CS, Bickler PE, Vexler ZS, Gregory GA. Neuroprotection and intracellular Ca^{2+} modulation with fructose-1,6-bisphosphate during in vitro hypoxia-ischemia involves phospholipase C-dependent signaling. Brain Res 2001;917:158–66.
Edde L, Zhou X, Eaton JW, Sherman MP. Induction of nitric oxide synthase in macrophages: inhibition by fructose-1,6-diphosphate. Biochem Biophys Res Commun 1998;243:683–7.
Ehringer WD, Niu W, Chiang B, Ou-Li W, Gordon L, Chien S. Membrane permeability of fructose-1,6-diphosphate in lipid vesicles and endothelial cells. Mol Cell Biochem 2000;210:35–45.
Espanol MT, Litt L, Hasegawa K, Chang LH, Macdonald JM, Gregory G, et al. Fructose-1,6-bisphosphate preserves adenosine triphosphate but not intracellular pH during hypoxia in respiring neonatal rat brain slices. Anesthesiology 1998;88:461–72.
Fahlman CS, Bickler PE, Sullivan B, Gregory GA. Activation of the neuroprotective ERK signaling pathway by fructose-1,6-bisphosphate during hypoxia involves intracellular Ca^{2+} and phospholipase C. Brain Res 2002;958:43–51.
Farias LA, Sun J, Markov AK. Improved brain metabolism with fructose 1–6 diphosphate during insulin-induced hypoglycemic coma. Am J Med Sci 1989;297:294–9.
Farias LA, Smith EE, Markov AK. Prevention of ischemic-hypoxic brain injury and death in rabbits with fructose-1,6-diphosphate. Stroke 1990;21:606–13.
Greco R, Mangione AS, Amantea D, Bagetta G, Nappi G, Tassorelli C. IkappaB-alpha expression following transient focal cerebral ischemia is modulated by nitric oxide. Brain Res 2011;1372:145–51.
Green LC, Wagner DA, Glogowski J, Skipper PL, Wishnok JS, Tannenbaum SR. Analysis of nitrate, nitrite, and [^{15}N]nitrate in biological fluids. Anal Biochem 1982;126:131–8.
Guha M, Mackman N. LPS induction of gene expression in human monocytes. Cell Signal 2001;13:85–94.
Han IO, Kim KW, Ryu JH, Kim WK. p38 mitogen-activated protein kinase mediates lipopolysaccharide, not interferon-γ, -inducible nitric oxide synthase expression in mouse BV2 microglial cells. Neurosci Lett 2002;325:9-12.
Hardin CD, Lazzarino G, Tavazzi B, Di Pierro D, Roberts TM, Giardina B, et al. Myocardial metabolism of exogenous FDP is consistent with transport by a dicarboxylate transporter. Am J Physiol Heart Circ Physiol 2001;281:H2654–60.
Hardin CD, Roberts TM. Metabolism of exogenously applied fructose 1,6-bisphosphate in hypoxic vascular smooth muscle. Am J Physiol 1994;267:H2325–32.
Hofer RE, Wagner SR, Pasternak JJ, Albrecht RF, Gallagher WJ, Lanier WL. Fructose-1,6-bisphosphate and fructose-2,6-bisphosphate do not influence brain carbohydrate or high-energy phosphate metabolism in a rat model of forebrain ischemia. J Neurosurg Anesthesiol 2009;21:31–9.
Izumi Y, Benz AM, Katsuki H, Matsukawa M, Clifford DB, Zorumski CF. Effects of fructose-1,6-bisphosphate on morphological and functional neuronal integrity in rat hippocampal slices during energy deprivation. Neuroscience 2003;116:465–75.
Juergens TM, Hardin CD. Fructose-1,6-bisphosphate as a metabolic substrate in hog ileum smooth muscle during hypoxia. Cell Biochem 1996;154:83–93.
Kaakinen T, Heikkinen J, Dahlbacka S, Alaoja H, Laurila P, Kiviluoma K, et al. Fructose-1,6bisphosphate supports cerebral energy metabolism in pigs after ischemic brain injury caused by experimental particle embolization. Heart Surg Forum 2006;9:E828–35.
Kelleher JA, Chan PH, Chan TY, Gregory GA. Energy metabolism in hypoxic astrocytes: protective mechanism of fructose-1,6-bisphosphate. Neurochem Res 1995;20:785–92.
Kim SH, Johnson VJ, Shin TY, Sharma RP. Selenium attenuates lipopolysaccharide-induced oxidative stress response through modulation of p38 MAPK and NF-kB signaling pathways. Exp Biol Med 2004;229:203–13.

Kleinert H, Pautz A, Linker K, Schwarz PM. Regulation of the expression of nitric oxide synthase. Eur J Pharmacol 2004;500:255–66.
Kuluz JW, Gregory GA, Han Y, Dietrich WD, Schleien CL. Fructose-1,6-bisphosphate reduces infarct volume after reversible middle cerebral artery occlusion in rats. Stroke 1993;24:1576–83.
Liu J, Hirai K, Litt L. Fructose-1,6-bisphosphate does not preserve ATP in hypoxic-ischemic neonatal cerebrocortical slices. Brain Res 2008;1238:230–8.
Long J, Zhang Z, Li X. The protective mechanism of fructose-1,6-diphosphate on ischemic brain injury. Zhonghua Yi Xue Za Zhi 2002;82:232–5.
Lopes RP, Lunardelli A, Preissler T, Leite CE, Alves-Filho JC, Nunes FB, et al. The effects of fructose-1,6-bisphosphate and dexamethasone on acute inflammation and T-cell proliferation. Inflamm Res 2006;55:354–8.
Minghetti L. Role of inflammation in neurodegenerative diseases. Curr Opin Neurol 2005;18:315–21.
Nathan C, Xie QW. Nitric oxide synthases: roles, tolls, and controls. Cell 1994;78:915–8.
Nishiya T, Uehara T, Edamatsu H, Kaziro Y, Itoh H, Nomura Y. Activation of Stat1 and subsequent transcription of inducible nitric oxide synthase gene in C6 glioma cells is independent of interferone-induced MAPK activation that is mediated by p21. FEBS Lett 1997;408:33–8.
Nogawa S, Zhang F, Ross ME, Iadecola C. Cyclo-oxygenase-2 gene expression in neurons contributes to ischemic brain damage. J Neurosci 1997;17:2746–55.
Ono K, Suzuki H, Sawada M. Delayed neural damage is induced by iNOS-expressing microglia in a brain injury model. Neurosci Lett 2010;473:146–50.
Pannu R, Singh I. Pharmacological strategies for the regulation of inducible nitric oxide synthase: neurodegenerative versus neuroprotective mechanisms. Neurochem Int 2006;49:170–82.
Park JY, Kim EJ, Kwon KJ, Jung YS, Moon CH, Lee SH, et al. Neuroprotection by fructose-1,6-bisphosphate involves ROS alerations via p38 MAPK/ERK. Brain Res 2004;1026:295–301.
Pawate S, Shen Q, Fan F, Bhat N. Redox regulation of glial inflammatory response to lipopolysaccharide and interferon. J Neurosci Res 2004;77:540–51.
Singh K, Balligand JL, Fischer TA, Smith TW, Kelly RA. Regulation of cytokine-inducible nitric oxide synthase in cardiac myocytes and microvascular endothelial cells. Role of extracellular signal-regulated kinases 1 and 2 (ERK1/ERK2) and STAT1 alpha. J Biol Chem 1996;271:1111–7.
Sola A, Berrios M, Sheldon RA, Ferriero DM, Gregory GA. Fructose-1,6-bisphosphate after hypoxic ischemic injury is protective to the neonatal rat brain. Brain Res 1996;741:294–9.
Song X, Wu B, Takata T, Wang X, Oizumi XS, Akisaki T, et al. Neuroprotective effect of D-fructose-1,6-bisphosphate against b-amyloid induced neurotoxicity in rat hippocampal organotypic slice culture: involvement of PLC and MEK/ERK signaling pathways. Kobe J Med Sci 2005;51:73–83.
Stringer JL, Xu K. Possible mechanisms for the anticonvulsant activity of fructose-1,6-diphosphate. Epilepsia 2008;49:101–3.
Sugimoto K, Iadecola C. Effects of aminoguanidine on cerebral ischemia in mice: comparison between mice with and without inducible nitric oxide synthase gene. Neurosci Lett 2002;331:25–8.
Tamaki T, Nakai T, Yamaue H. Fructose-1,6-bisphosphate inhibits excess activation of Kupffer cell function induced by endotoxin. Dig Dis Sci 2002;47:2179–85.
Tang XY, Zhang Q, Dai DZ, Ying HJ, Wang QJ, Dai Y. Effects of strontium fructose 1,6-diphosphate on expression of apoptosis-related genes and oxidative stress in testes of diabetic rats. Int J Urol 2008;15:251–6.
Trimarchi GR, Arcadi FA, Imperatore C, Ruggeri P, Costa G. Effect of fructose-1,6-biphosphate on microsphere-induced cerebral ischemia in the rat. Life Sci 1997;61:611–22.
Vexler ZS, Wong A, Francisco C, Manabat C, Chriten S, Tauber M, et al. Fructose-1,6-bisphosphate preserves intracellular glutathione and protects cortical neurons against oxidative stress. Brain Res 2003;960:90–8.
Xu K, Stringer JL. Pharmacokinetics of fructose-1,6-diphosphate after intraperitoneal and oral administration to adult rats. Pharmacol Res 2008;57:234–8.